Thermal Creep and Stress Relaxation of London Clay

Bradley Sheridan[1], Meghdad Bagheri[2], Mohammad Rezania[3]

Abstract

This paper investigates the effect of temperature variations on the creep and stress relaxation behaviour of clay samples from London Bank Station. The independent and coupled effects of strain-rate and temperature on one-dimensional stress-strain and stress relaxation responses were investigated based on a series of temperature-controlled constant rate of strain (CRS) compression-relaxation tests carried out at fast, intermediate, and slow displacement-rates and over a temperature range of 20 - 55°C. The temperature effect on creep index (C_α) was investigated based on a series of temperature-controlled multi-staged loading (MSL) oedometer tests. The results of CRS compression-relaxation tests showed that with the increase of temperature, the coefficient of stress relaxation (R_α) decreases for samples loaded at fast and intermediate pre-relaxation displacement-rates ($\dot{v}$), but it increases for samples loaded at the slow pre-relaxation displacement-rate. A decrease in $\dot{v}$ by a factor of 10, i.e. from 0.01 to 0.001 mm/min, causes the R_α values to reduce by 55 – 11% with temperature increase. The increase in temperature was found to generally cause an increase in C_α values obtained from the MSL tests. The maximum value of C_α increased by 18% for temperature change from 35°C to 45°C, and by 37% for temperature change from 45°C to 55°C. The temperature effects on other conventional parameters including preconsolidation pressure, compression and swelling indices (C_c and C_s) were found to be comparable with findings reported in the literature. Comparing the values of C_α obtained from the MSL tests, and R_α values obtained from the CRS tests supports the validity of $R_\alpha = C_\alpha/C_c$ correlation for thermally influenced saturated reconstituted clays, and that the time-dependent soil parameters could be obtained from relatively fast CRS compression-relaxation tests as an alternative to conventional time-consuming oedometer tests.

Keywords: Creep, Stress relaxation, Temperature effect, London Clay

[1]PhD Student, Warwick Institute for the Science of Cities, University of Warwick, Coventry, UK.
Email: B.Sheridan@warwick.ac.uk

[2]Lecturer, School of Energy, Construction and Environment, Coventry University, Coventry, UK.
Email: ac6031@coventry.ac.uk. ORCID: https://orcid.org/0000-0002-9748-4165

[3]Reader, School of Engineering, University of Warwick, Coventry, UK. (Corresponding Author)
Email: m.rezania@warwick.ac.uk. ORCID: https://orcid.org/0000-0003-3851-2442

Introduction

In the context of environmental and energy geotechnics, a deep understanding of the thermo-hydro-mechanical (THM) behaviour of soils, in particular clays, is necessary for design and analysis of geotechnical problems including energy or heat exchanger piles, high voltage electricity cable burials, and landfill liners. Many studies have been carried out to investigate the thermo-mechanical behaviour of clays (Campanella and Mitchell, 1968; Tidfors and Sällfors, 1989; Jarad et al., 2019; Kaddouri et al., 2019; Loria and Coulibaly, 2021; Lahoori et al., 2021). However, the reported findings on the thermally influenced behaviour including volume change, yielding, and compressibility are often inconsistent and inconclusive. For example, Campanella and Mitchell (1968), Delage et al. (2000), and Kaddouri et al. (2019) reported negligible impact of temperature on the compression index (C_c) and swelling index (C_s) parameters of compacted clays. Similarly, Martinez Calonge (2017) reported temperature independency of compression index for London clay (LC) samples. However, thermal variations of C_c and C_s were reported respectively in the works of Tsutsumi and Tanaka (2012) and Abuel-Naga et al. (2007). The general consensus in the literature is that the yield stress for clays decreases with increase in temperature (e.g. Tidfors and Sällfors, 1989; Boudali et al., 1994; Kaddouri et al., 2019; Cheng et al., 2020; Chen et al., 2023). However, few studies have reported an increase in yield stress with temperature (e.g. Sultan et al., 2002). The thermal behaviour of saturated clays depends on many factors including; stress history, overconsolidation ratio (OCR), thermo-mechanical stress path, specimen preparation method, and soils' structure, plasticity, and mineralogy. These factors may be considered as the underlying reasons for the above contradictions reported in the literature.

In many cases, including buried high voltage electricity cables and thermal energy storage systems, clayey soils are exposed to elevated temperatures for a long period, arising the need for better understanding the time-dependent behaviour of these soils. Despite various studies

on the THM behaviour of clays, few works have investigated thermal effects on long-term behaviour, mainly creep and stress relaxation. Jarad (2016) studied the thermal effects on compacted clays and reported an increase in creep rate (C_α) with temperature increase. This observation was attributed to the reduction in apparent viscosity of the contacts between the particles at higher temperatures. Li et al. (2018) noted in a study on Swedish sensitive clays that creep rate is temperature- and stress-dependent, and largely affected at stress levels above the apparent pre-consolidation pressure. Li et al. (2018) reported that the increase of C_α is due to soil structure variations as the result of microstructural water transfer at the inter-particle links. The dependency of C_α to stress and temperature was also reported in the works of Kaddouri et al. (2019) on compacted clayey soils. The authors found that the values of C_α were more significant at higher stresses and higher temperatures. At a given stress level, the increase in C_α with temperature change from 5°C to 70°C was mainly deemed to be caused by the reduction in viscosity of the soil skeleton and pore-water at high temperatures. Despite the above findings of the temperature dependency of C_α, the works of Marques et al. (2004) on Champlain Sea clays and Di Donna and Laloui (2015) on silty clay from Switzerland conclude C_α to be temperature independent.

According to Ladanyi and Benyamina (1995), investigation of creep behaviour can be done more conveniently by conducting stress relaxation tests rather than conventional creep tests. During a creep test, a constant load is maintained and variation of strain with time is recorded. Whereas, in a relaxation test, an initial strain level is maintained and the decay of stress with time is monitored. During a creep test, the soil structure changes with time, sometimes in an unpredictable manner. Whereas, in a relaxation test, the internal soil structural changes remain very small and only internal stresses redistribute from an elastic to an inelastic state (Ladanyi and Benyamina, 1995). The soil's behaviour may therefore be considered more predictable during a stress relaxation test than a creep test. Yin et al. (2014) proposed that the

correlation $R_\alpha = C_\alpha/C_c$ (R_α is the coefficient of stress relaxation) can be used for determination of creep index from stress relaxation results. Bagheri et al. (2019b) and Bagheri and Rezania (2021) studied the stress relaxation behaviour of saturated and unsaturated reconstituted LC specimens. Their study found a clear dependency of R_α to pre-relaxation strain and strain-rate and validated the $R_\alpha = C_\alpha/C_c$ relationship for the limited ranges of suction and stresses applied. To the best of the authors' knowledge, there are no reported studies that investigated the influence of temperature on stress relaxation behaviour of clays.

This paper presents an experimental study on the influence of temperature on stress relaxation, creep, and compression behaviour of reconstituted saturated LC over a temperature range of 20°C to 55°C. The influence of temperature and displacement-rate on compression-relaxation response is analysed by a series of constant rate of strain (CRS) oedometer tests using an advanced temperature-controlled CRS oedometer apparatus. Furthermore, a series of temperature-controlled multi-staged loading (MSL) oedometer tests are performed to investigate creep and compression response under non-isothermal conditions.

Test Material

The material used in this study is London clay, which was collected from the Bank Station upgrade project in London, UK. The material's index parameters and physical properties are shown in Table 1. The test specimens were prepared following the procedure outlined in Rezania et al. (2020). Initially, the disturbed samples were oven-dried for a minimum of 48 hours to release the moisture, then crushed into powder and sieved through a 1.18 mm opening sieve. The sieved material was mixed with deaired distilled water at 1.5 times the liquid limit (w_L). The soil slurry was then consolidated in a 120 mm diameter Perspex consolidometer under a vertical stress of 75 kPa for five days. The samples were then quickly unloaded to minimise swelling and water absorption. Finally, the test specimens were cored from the soil

cake using a 95 mm diameter and 35 mm height cutting ring and a conventional oedometer

ring of 75 mm diameter and 20 mm height.

Table 1 - Physical properties of Bank Station London clay specimens

Property	Value
Grain size, D (mm), 0.6 mm < D < 1 mm	5%
Grain size, D (mm), 0.063 mm < D < 0.6 mm	76%
Grain size, D (mm), D < 0.063 mm	19%
Plastic Limit, w_P	24%
Liquid Limit, w_L	77%
Plasticity Index, I_P	53
Specific Gravity, G_s	2.69

Test Apparatus

Temperature-controlled Oedometer Cells

A set of three conventional oedometer cells were modified to accommodate a simple

temperature control system allowing for investigating the combined effect of temperature and

applied vertical stress on both primary and secondary consolidation behaviour of the specimens

during multi-staged loading (MSL) tests. The temperature control system consists of an RS

PRO silicone heater mat, a voltage supply, and a digital J-type thermocouple thermometer. The

heater mat placed at the base of the oedometer cell provides the required heating. The

specimen's temperature was constantly monitored through a J-type thermocouple placed inside

the cell and close to the soil specimen. It is assumed that temperature distribution over the

specimen is uniform given the specimen submergence in pre-heated water and

interconnectivity of pore-water. Figure 1 presents a schematic diagram of the temperature-

controlled oedometer test setup.
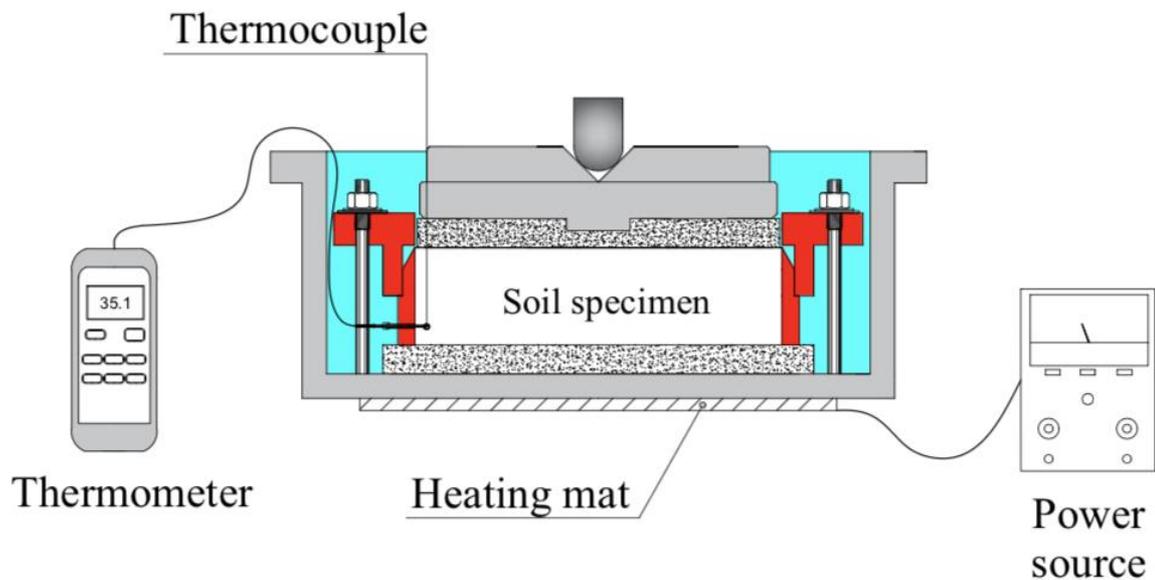
Figure 1 – Schematic diagram of the temperature-controlled oedometer cell

Temperature-controlled CRS Oedometer Cell

The temperature-controlled CRS oedometer cell designed at the University of Warwick (Bagheri et al., 2019a) was used for conducting the thermal CRS compression and relaxation tests. In this equipment, the test specimen is placed in a 95 mm diameter and 35 mm height ring and sandwiched between two porous stones providing drainage at the top and bottom of the specimen. Pore-water pressure is measured using a pressure transducer connected to the base of the specimen. Axial force is applied using a load frame, compressing the specimen at a pre-defined displacement-rate, and measured by a 25 kN submersible load cell. The vertical deformation is measured by a 25 mm linear potentiometric transducer (LPT) with an accuracy of 0.001 mm. A WATROD double-ended tubular heater element, placed at the base of the cell, is used for heating up the cell and the specimen. A temperature control unit is also used to continuously monitor the set target temperature and the actual applied temperature to the specimen based on the feedback from two J-type thermocouples connected to the cell's body

and the specimen. It must be noted that the thermal expansion or contraction of the cutting ring

has a negligible impact on the oedometric condition (François and Laloui, 2010), and hence,

disregarded in correction of the obtained vertical deformations. The method proposed by

Bagheri et al. (2019a) was followed to correct the measured axial deformations for the

thermally induced deformation of the cell structure. Figure 2 presents a schematic diagram of

the temperature-controlled CRS oedometer system setup.
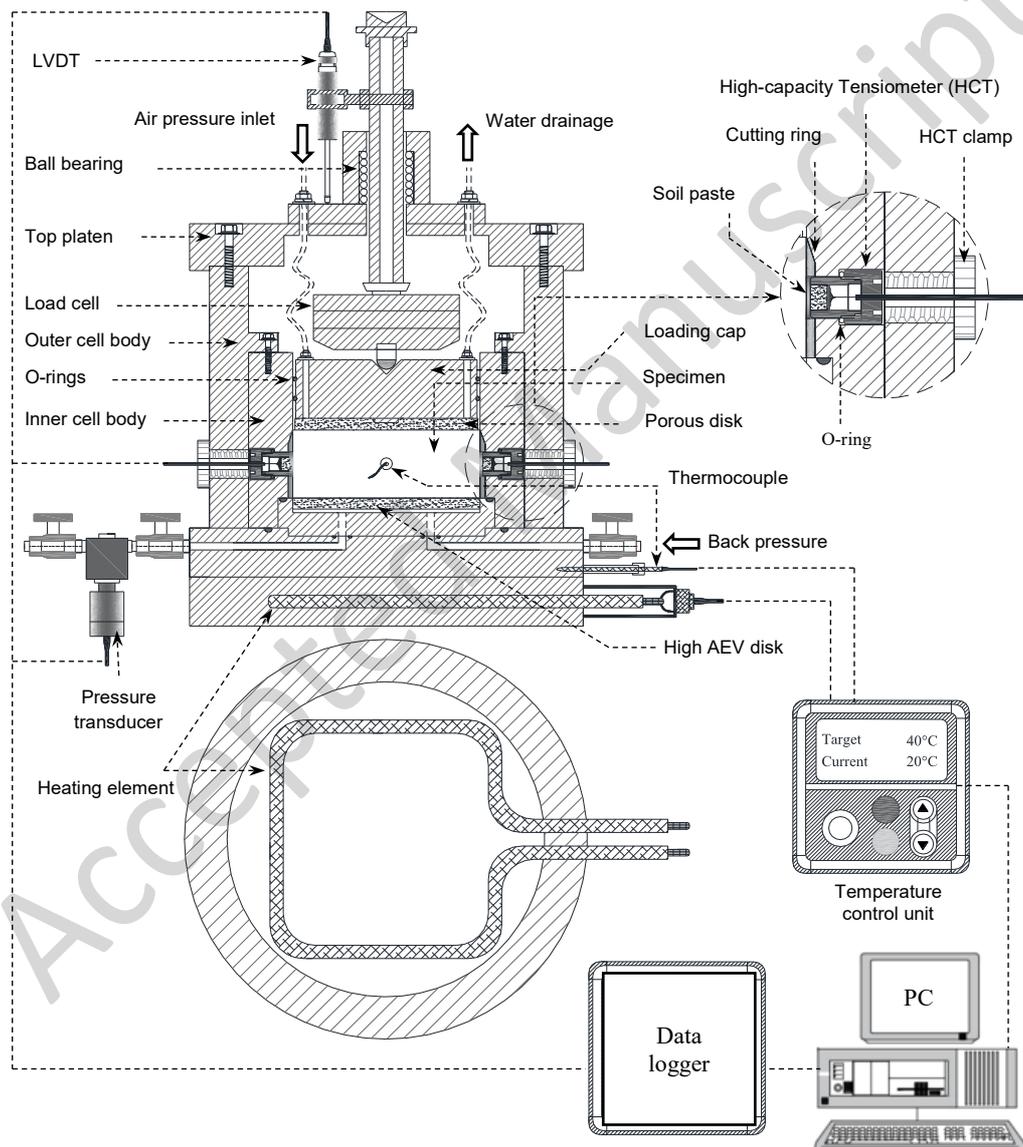
Figure 2 – Schematic diagram of the temperature-controlled CRS oedometer system

Experimental Program

A total of eight saturated MSL oedometer tests with 24 hour loading periods were performed on reconstituted specimens at four different temperatures of 20, 35, 45, and 55°C. In practice, the temperature in liners of wet landfills has been reported to be within a range of 40 to 60°C (Rowe, 2012). Energy piles have been reported to typically experience temperatures ranging from 10 to 35°C under monotonic heating and cooling (McCartney and Murphy, 2017). This justifies the selection of 20 to 55°C temperature range in this study. Furthermore, the selected temperature range is in compliance with the common temperature ranges selected in the reported works in the literature (e.g. Favero et al., 2016; Bagheri et al., 2019a).

Prior to the start of the tests, the initial water content (w_0) and the specimen dimensions were measured. The specimen was then placed in the temperature-controlled oedometer cell and heated to the desired temperature. Once thermal equilibrium between the heating system and the specimen was achieved, the vertical load was applied incrementally to the submerged specimen. The heating was maintained constant throughout the experiment and any loss of water from the cell due to the evaporation was compensated by topping up the cell with water pre-heated to the test temperature. By the end of loading, the specimen was unloaded step-wise to evaluate the swelling response. The compression curve was finally obtained based on final settlement values. The tests were conducted twice at the same initial conditions to ensure the repeatability and reliability of the results. This set of experiments allows for investigation of the temperature effects on compression index (C_c), swelling index (C_s), and the creep index (C_α). Table 2 outlines the details of the MSL tests. Each test is comprised of eight stages of loading and four stages of unloading with a total test time of 12 days.

Table 2 - Details of MSL oedometer tests

Test ID	Temperature (°C)	w_0 (%)
MSL20-1	20	39
MSL20-2	20	39
MSL35-1	35	39
MSL35-2	35	39
MSL45-1	45	39
MSL45-2	45	39
MSL55-1	55	39
MSL55-2	55	39

A total of 12 saturated compression-relaxation CRS oedometer tests were carried out on reconstituted specimens at four different temperatures of 20, 35, 45, and 55°C and three different displacement-rates ($\dot{v}$) of 0.01, 0.005, and 0.001 mm/min. The selection of the displacement-rates was based upon the pore pressure ratio (PPR) of 3 – 15% according to ASTM-D4186 (ASTM, 2006). PPR is the ratio of excess pore-water pressure (u_{exc}) to the applied vertical stress (σ_v). Prior to the tests, the water content (w_0) and the specimen dimensions were measured. The cell was prepared following the procedure outlined in Bagheri et al. (2019a). The specimen confined within the cutting ring was placed in the cell and an initial vertical stress of 10 kPa was applied to avoid any possible bedding effects. The CRS tests comprised of two stages: i) loading the specimen at a constant rate of displacement to the maximum load capacity of the cell ($\cong$ 3500 kPa) and ii) stress relaxation at zero rate of axial displacement for 48 hours. This set of experiments allows for investigation of temperature and displacement-rate effects on the compression and stress relaxation processes. Table 3 outlines the details of these tests.

Table 3 - Details of compression-relaxation CRS oedometer tests

Test ID	Temperature (°C)	Displacement rate (mm/min)	Maximum vertical stress (kPa)	PPR (%)	Duration of compression stage (minute)
CRS20-a	20	0.01	3329	14.61	1130
CRS20-b	20	0.005	3498	10.22	2440
CRS20-c	20	0.001	3376	5.12	10530
CRS35-a	35	0.01	3300	13.06	1180
CRS35-b	35	0.005	3466	10.04	2270
CRS35-c	35	0.001	3350	5.78	10890
CRS45-a	45	0.01	3197	12.48	1010
CRS45-b	45	0.005	3493	8.63	2260
CRS45-c	45	0.001	3401	4.74	11760
CRS55-a	55	0.01	3196	12.50	920
CRS55-b	55	0.005	3495	6.43	2720
CRS55-c	55	0.001	3450	4.86	12360
a, b, and c = displacement rates					

Parameters

In the MSL oedometer tests the compression index (C_c), swelling index (C_s), and reloading index (C_r) were calculated as the slope of respectively normal consolidation line (NCL), swelling (unloading) line, and reloading line in $e - log\sigma'_v$ plot. Apparent preconsolidation pressure (σ'_p) was obtained based on the Casagrande method, and the incremental creep index (C_α) was calculated as the slope of the linear part of the $e - logt$ plot corresponding to time interval of 6 – 24 hours for each load increment since the primary consolidation was found to be completed within the first 5 – 6 hours.

In the CRS oedometer tests, the C_c value is calculated as the slope of the NCL, and the yield vertical net stress (σ_p) is determined as the intersection of the best-fitted lines to the pseudoelastic and plastic sections of the compression curve. The stress relaxation process was evaluated using three main parameters: the coefficient of relaxation (R_α), relaxed stress ($\Delta\sigma$), and the residual stress ratio (ξ). In stress relaxation stage of the CRS tests, the value of R_α can

be determined as the slope of the plot of total vertical stress (σ_v) versus time (t) in $log\sigma_v - logt$ space

$$R_\alpha = -\frac{\Delta\log(\sigma_v)}{\Delta\log(t)} \tag{1}$$

The relaxed stress ($\Delta\sigma$) is defined as

$$\Delta\sigma = \sigma_0 - \sigma_s \tag{2}$$

The stress value at the end of the relaxation course is known as the residual total vertical stress (σ_s). The ratio of σ_s to pre-relaxation total vertical stress (σ_0) is defined as the residual stress ratio

$$\xi = \frac{\sigma_s}{\sigma_0} \tag{3}$$

Discussion of Results

Evaluation of Overall Compressibility in Thermal MSL Tests

Figure 3 presents the compression curves in the $e/e_0 - log\sigma_v'$ space where e/e_0 is the normalised void ratio with respect to initial void ratio (e_0). As it can be seen, with increase in temperature, the overall compressibility of the specimens is increased exhibiting higher deformations at a given vertical effective stress. In the literature, this has been explained with the hypothesis of thermal softening at higher temperatures whereby the temperature-induced change in viscosity of pore-water weakens the inter-particle contact forces leading to higher deformability characteristics (Kaddouri et al. 2019, Lahoori et al. 2021). It should be noted that the increase in compressibility with increase in temperature is more pronounced at higher stress levels.

11
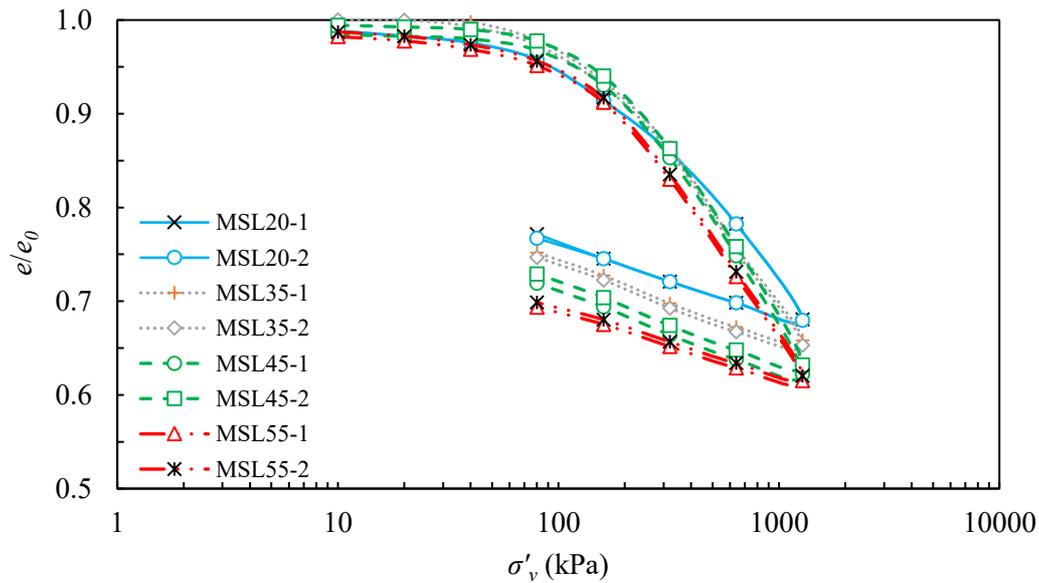
Figure 3 - Compression curves at different temperatures for the MSL oedometer tests

Variation of compression and swelling indices with temperature is shown in Figure 4. Inspection of the results shows minimal impact of temperature on C_c and C_s values at the tested temperatures, despite the overall increase in compression response with temperature. Figure 5 presents the variation of σ'_p with temperature. There appears to be a reduction of σ'_p values with temperature that follows approximately a linear trend ($R^2 = 0.95$). Thermal softening and potential reduction in adsorbed water of clay particles are the possible reasons for reduction in σ'_p with temperature.
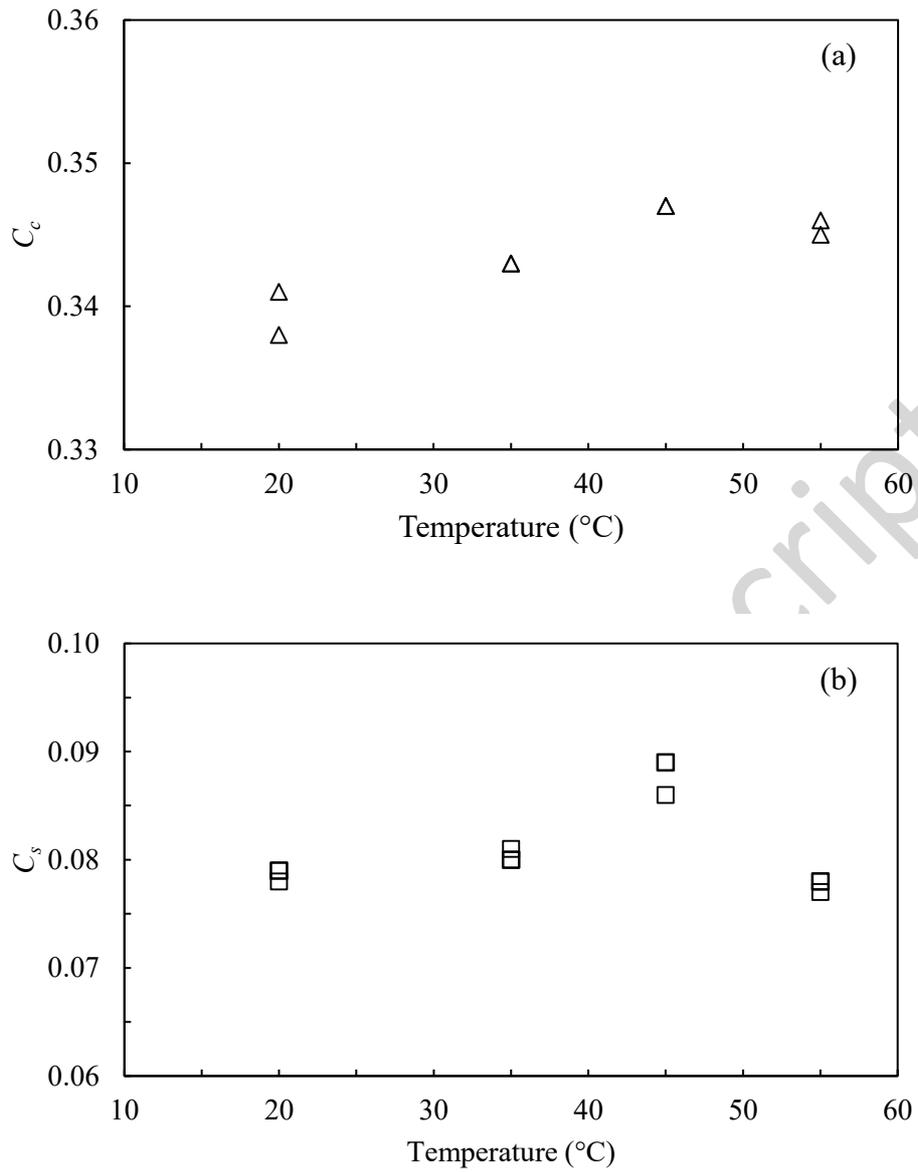
Figure 4 - Effect of temperature on the compression index (a) and swelling index (b) in MSL

tests
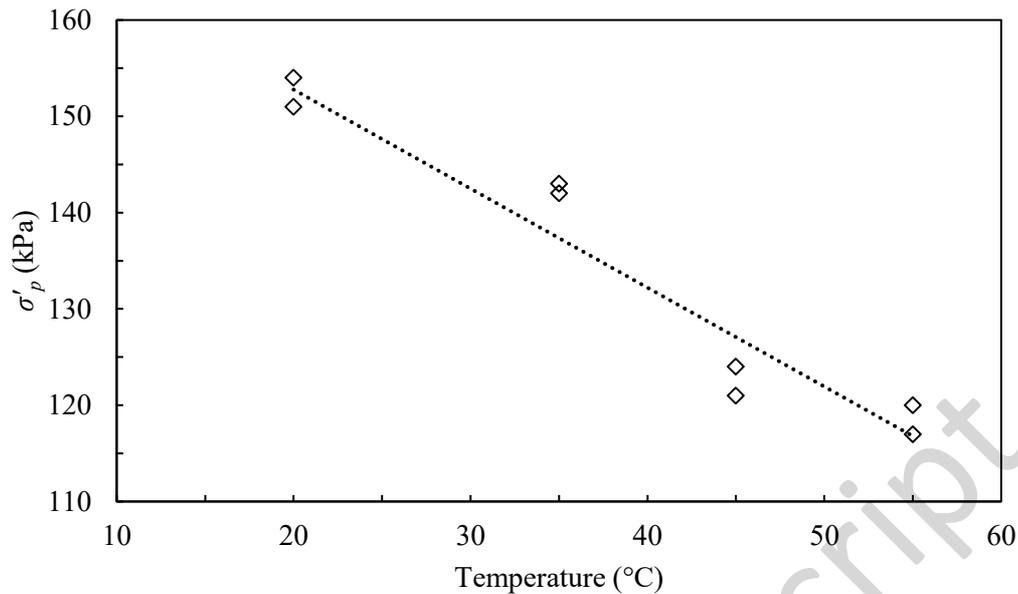
Figure 5 - Effect of temperature on σ'_p in MSL tests

Temperature- and Stress-dependent Response in Thermal MSL Tests

Figure 6 shows the variation of the slope of the compression curve (m_c) with the normalised

stress σ'_v/σ'_p . The values of m_c were calculated as $\Delta e/\Delta log\ \sigma'_v$ for each loading increment of

the MSL tests. As it can be seen, prior to σ'_p, the $m_c = C^*_r$ values (where C^*_r is the incremental

recompression index) increase slightly. Following σ'_p, the $m_c = C^*_c$ values (where C^*_c is the

incremental compression index) increase gradually up to a peak value at around (4-5) σ'_p, after

which a decrease in compressibility is observed. The rate of increase in C^*_c with stress level

appears to be almost the same for specimens tested at different temperatures. Temperature does

not seem to have a significant impact on the C^*_r values in overconsolidation region, although a

slight reduction is observed as stress level approaches the yield stress. However, in post yield

region, the C^*_c values appear to generally decrease with increase in temperature. This might be

an indication of predominant effect of stress level on the compressibility response.
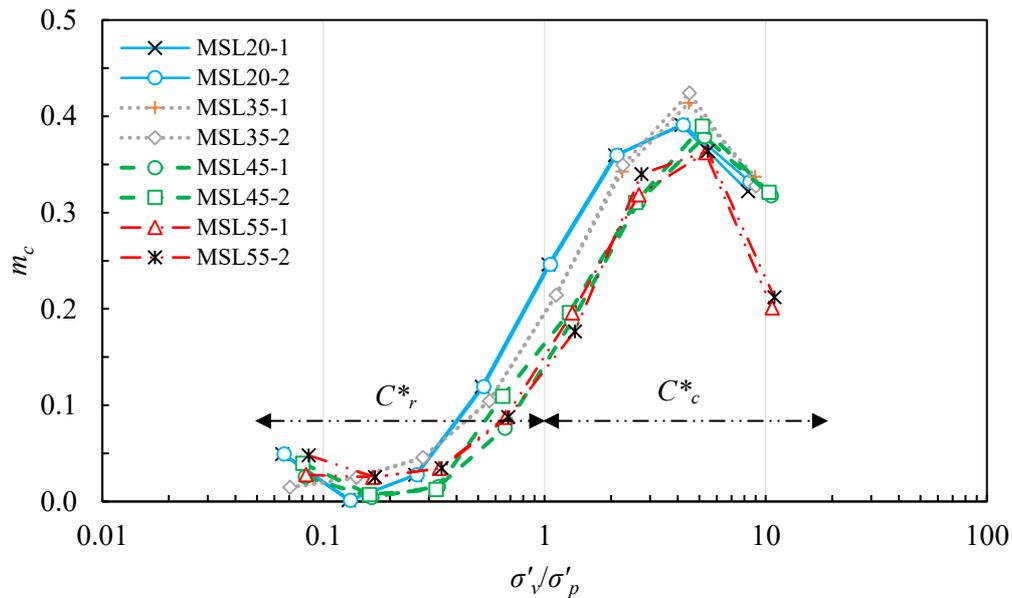
Figure 6 – Stress dependency and temperature dependency of m_c in MSL oedometer tests

Figure 7 presents the variation of C_α with σ'_v and temperature. The values of C_α increase with increase in vertical effective stress to a peak value, then decrease. Temperature appears to have a notable impact on creep index especially at higher stress levels and higher temperatures in the post yield region. The maximum value of C_α increased by 18% for temperature change from 35°C to 45°C, and by 37% for temperature change from 45°C to 55°C. At higher temperatures, the viscosity of pore-water is reduced. This may result in potential microstructural variations due to migration of pore-water to inter-aggregate space, hence observation of higher creep rate. The potential pore-water transfer between intra-aggregate and inter-aggregate space could be further facilitated by the application of higher stresses in the post-yield region. Further inspection of the results revealed slight impact of temperature on C_α in elastic domain ($\sigma'_v/\sigma'_p < 1$). However, with the scatter of data points, it is not possible to comment whether temperature gradient increases or decreases C_α in this region. Despite the clear impact of temperature in post-yield region, with limited data it is hard to make a firm conclusion on overall variation of C_α with temperature.
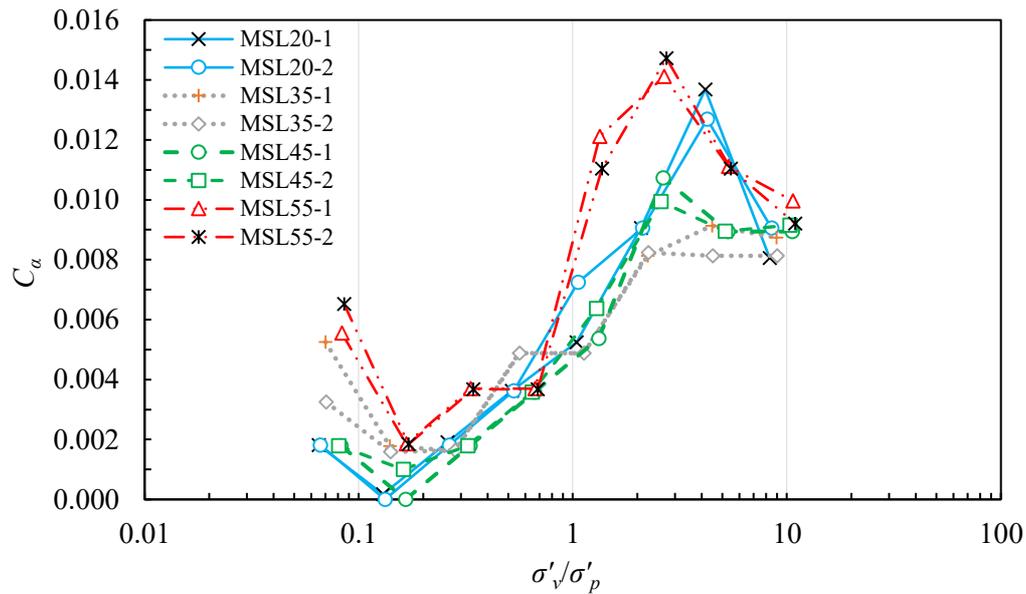
Figure 7 – Stress dependency and temperature dependency of C_α in MSL oedometer tests

The ratio of $\alpha = C_\alpha/m_c$ provides an additional analysis of temperature and stress level effects on one-dimensional compression. As it can be seen in Figure 8, the values of α decrease gradually as stress levels increase. The effect of temperature appears to be more pronounced at lower stress levels and before the yield stress. The predominant trend in the post peak region suggests convergence of α towards a fixed value of approximately 0.029.
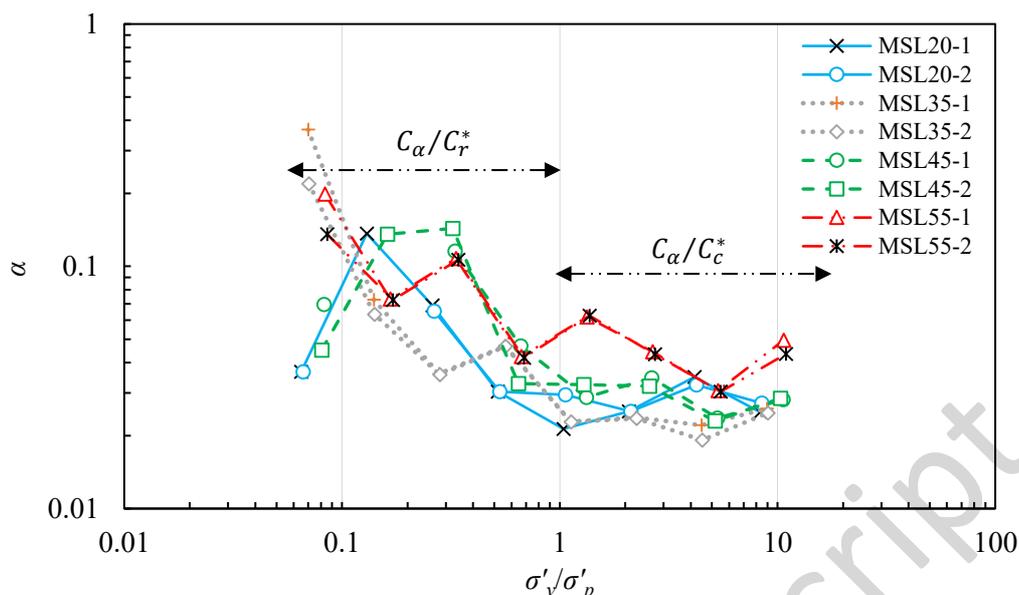
Figure 8 - Stress dependency and temperature dependency of α in MSL oedometer tests

Influence of Temperature and Displacement-rate on Stress-Strain Response in Thermal CRS Tests

Figure 9 shows the stress-strain response in $\varepsilon_a - log\sigma_v$ space for the compression stage of the thermal CRS tests carried out at three different displacement-rates, along with evolution of generated excess pore-water pressure (u_{exc}). For the tests carried out at fast displacement-rate (0.01 mm/min), the effect of temperature appears to be marginal (Figure 9a). At intermediate displacement rate (0.005 mm/min) however, the increase in temperature resulted in higher compressibility response and shift of the compression curves to the left (Figure 9b). This impact on the specimens tested at slow displacement rate (0.001 mm/min) was only evident at higher stress levels and generally beyond the yield stress (Figure 9c). This might be attributed to the gradual development of inter-particle bonding due to aging effect, leading to a shift of the compression curves to the right. Inspecting the variation of u_{exc} with σ_v reveals that the higher the displacement rate, the higher the generated u_{exc}. The rate of change of u_{exc} was also found to generally decrease with an increase in temperature.
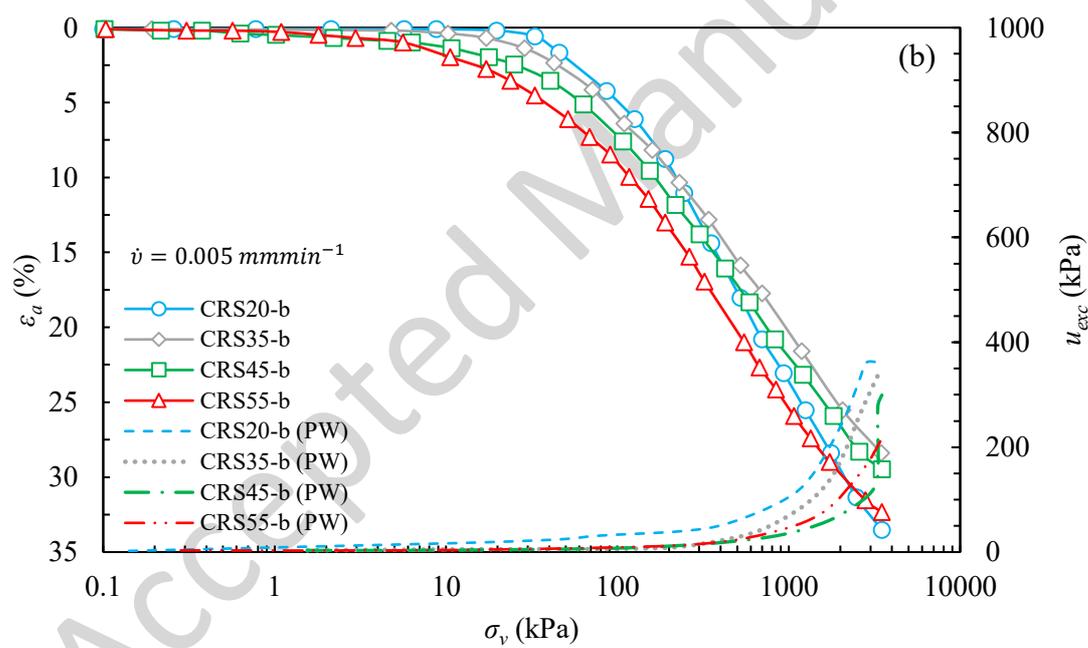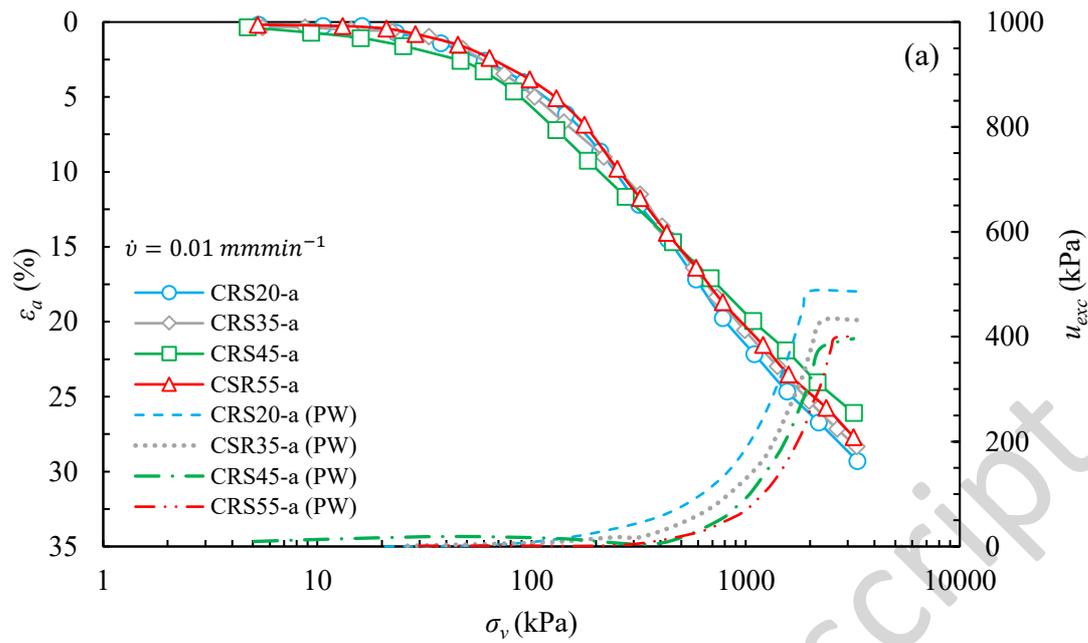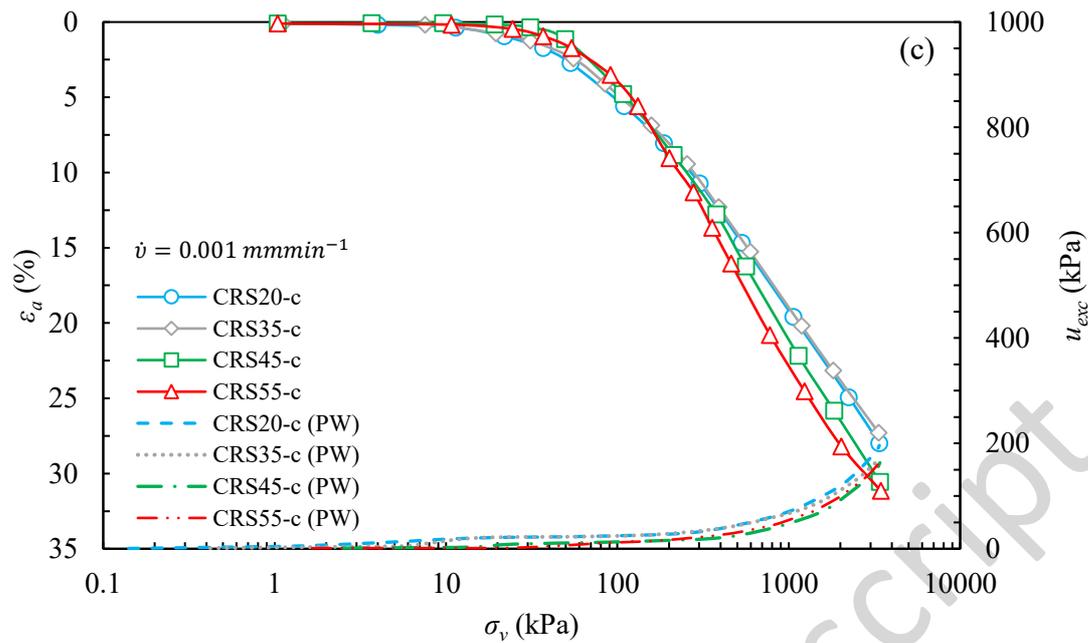
Figure 9 - CRS compression curves at different temperatures for displacement rates of: (a) 0.01mm/min; (b) 0.005mm/min; and (c) 0.001mm/min.

Figure 10 illustrates the variation of C_c with temperature for the three sets of thermal CRS tests carried out at different displacement-rates of 0.01 mm/min (a), 0.005 mm/min (b), and 0.001 mm/min (c). It is observed that at a fixed temperature, the values of C_c increase with the decrease in displacement-rate. Furthermore, at a fixed displacement-rate, the values of C_c appear to decrease approximately linearly with increase in temperature. For the limited range of the applied vertical stresses, the effect of displacement-rate on compression index prevails and is more pronounced. For instance, a 20% increase of C_c obtained due to a 10-fold decrease of $\dot{v}$ from 0.01 to 0.001 mm/min, which is significantly higher than the 9% decrease of C_c values with increasing the temperature from 22 to 55°C for the tests carried out at fixed displacement-rate of 0.001 mm/min.
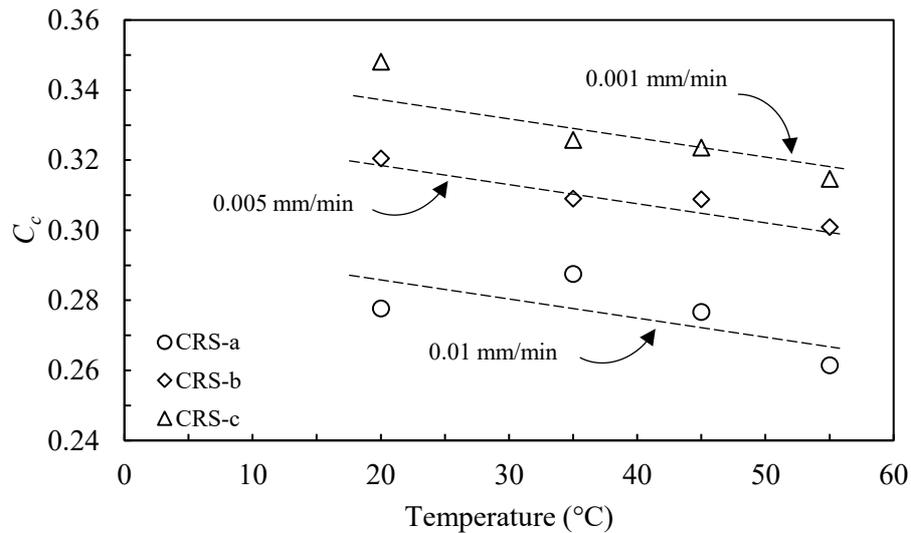
Figure 10 - Effect of temperature and displacement-rate on C_c in CRS tests

Figure 11 presents the variation of σ_p with temperature for the three sets of thermal CRS tests carried out at different displacement-rates. It is observed that at a fixed temperature, the values of σ_p increase with increase in displacement-rate. Furthermore, at a fixed displacement-rate, the values of σ_p appear to decrease with increase in temperature. Further inspection of the results revealed that a 10-fold increase of displacement-rate from 0.001 to 0.01 mm/min resulted in 11%, 8%, 9%, and 7% reduction of σ_p for the tests carried out under constant temperatures of 20, 35, 45, and 55°C respectively. Similarly, the values of σ_p were found to decrease by 17%, 16%, and 13% for test carried out under constant displacement-rate of 0.01, 0.005, and 0.001 mm/min respectively. Based on these observations and within the considered ranges of temperatures and displacement-rates in this study, one may conclude that the effect of displacement-rate on σ_p prevails and is more pronounced in comparison with temperature. Furthermore, σ_p appears to follow an approximately linear trend with temperature for all three different displacement-rates considered in this study.
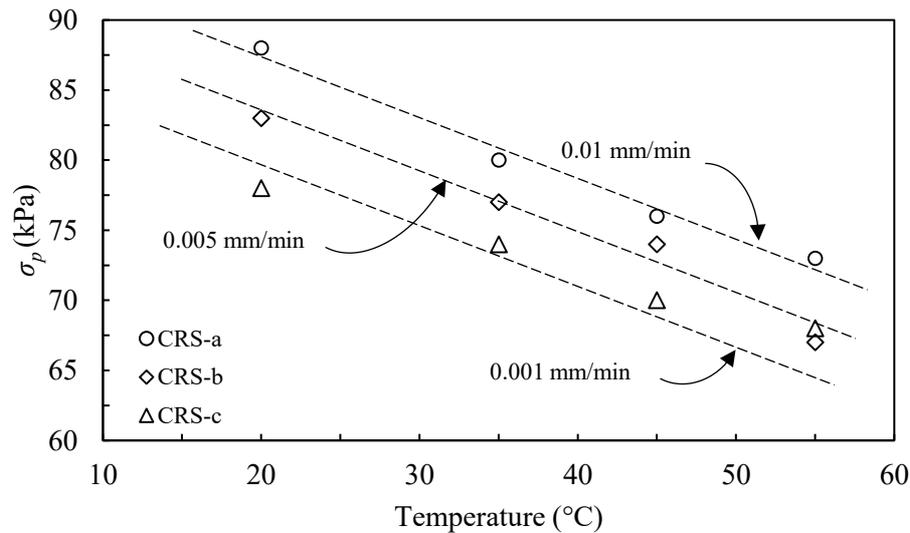
Figure 11 - Effect of temperature and displacement-rate on σ_p in thermal CRS tests

Influence of Temperature and Displacement-rate on Stress Relaxation Response in Thermal CRS Tests

The stress relaxation process was initiated right after the specimens which had been loaded at different displacement-rates, reached the maximum vertical stresses listed in Table 3. The gradual decrease of stresses and excess pore-water pressure (u_{exc}) were recorded and used to evaluate the effects of pre-relaxation displacement-rate and temperature on the stress relaxation process. Table 4 summaries the characteristics and results of 48 hours thermal relaxation tests. Considering the values of relaxation parameters in Table 4, it is found that an increase in temperature from 20 to 55ºC generally causes a decrease in relaxed stresses ($\Delta\sigma$) and consequently an increase in the stress relaxation ratio (ξ) in tests carried out at fast (0.01 mm/min) and intermediate (0.005 mm/min) displacement-rates, producing a reduction of 72% and 35% in $\Delta\sigma/\sigma_0$ ratio respectively. This could be attributed to the accumulation of less strain energy within the specimens during fast loading caused by weakening the bonds between the particles as temperature increases. In other words, the reduction in viscosity of water at higher temperatures facilitates straining and release of accumulated energy during the loading stage. On the other hand, prolonging the pre-relaxation loading stage may result in a portion of the

21

absorbed thermal energy to be used for further weakening or breaking the existing inter-particle bonds, and therefore, accumulation of significantly lower strain energy in the system. Temperature appears to have marginal impacts on the stress relaxation process in tests carried out at low displacement-rate (0.001 mm/min). No trend was observed in variation of $\Delta\sigma$, $\Delta\sigma/\sigma_0$ ratio, and ξ in the CRS-c tests.

Table 4 - Characterisation of the stress relaxation parameters

Test ID	T (ºC)	σ_0 (kPa)	σ_s (kPa)	$\Delta\sigma$ (kPa)	$\Delta\sigma/\sigma_0$ (%)	ξ	R_α
CRS20-a	20	3329	1776	1553	46	0.53	0.046
CRS35-a	35	3300	2231	1069	32	0.67	0.042
CRS45-a	45	3197	2734	463	14	0.85	0.040
CRS55-a	55	3196	2753	443	13	0.86	0.034
CRS20-b	20	3498	2465	1033	29	0.70	0.038
CRS35-b	35	3466	2611	855	24	0.75	0.037
CRS45-b	45	3493	2700	793	22	0.77	0.034
CRS55-b	55	3495	2810	685	19	0.80	0.034
CRS20-c	20	3376	3086	290	8	0.91	0.021
CRS35-c	35	3350	3084	266	7	0.92	0.022
CRS45-c	45	3401	3132	269	7	0.92	0.025
CRS55-c	55	3450	3135	315	9	0.90	0.030

Figure 12 presents the relaxation of vertical stress with time on a semi-log plot of σ_v/σ_0 versus time, where σ_v/σ_0 is the normalised relaxed stress with respect to pre-relaxation stress (σ_0). Also shown in the graphs are the variations of u_{exc} with time during the stress relaxation stage. For the tests carried out under fast and intermediate pre-relaxation loading rates, the increase in temperature resulted in a decrease in the rate and magnitude of relaxed stresses, whereas for the tests carried out at slow pre-relaxation loading rate, the opposite is observed. Bagheri et al. (2019b) showed that the stress relaxation process involves three distinct phases of fast relaxation, decelerating relaxation, and residual relaxation. Inspection of the graphs of Figure 12 reveals that such phases are more evident in tests carried out at lower temperatures and faster pre-relaxation loading rates. Apparently, with increase of temperature and pre-relaxation

loading rate, the curvature of the stress relaxation curves is gradually faded resulting in almost a linear variation of relaxed stresses with logarithm of time. A sudden decrease of the relaxed stress observed in CRS20-a test compared to CRS45-a and CRS55-a tests might be associated with a quick release of the high amount of strain energy stored inside the specimen during the loading stage at room temperature (20°C). The relaxation curve for this test is therefore characterised with a higher (steeper) gradient. Similar observations were reported by Bagheri et al. (2019b) in 1D compression-relaxation tests on Sheppey London Clay.

To further investigate the relaxation process in thermal CRS tests, the results of tests carried out at constant temperature (different displacement-rates) are compared in graphs of Figure 13. It is observed that, at a constant temperature, the rate and magnitude of the relaxed stresses increase with increase in pre-relaxation loading rate for tests carried out at 20 and 35°C. This is not, however, the case for tests carried out at 45 and 55°C where negligible change in the rate of relaxed stresses is observed.
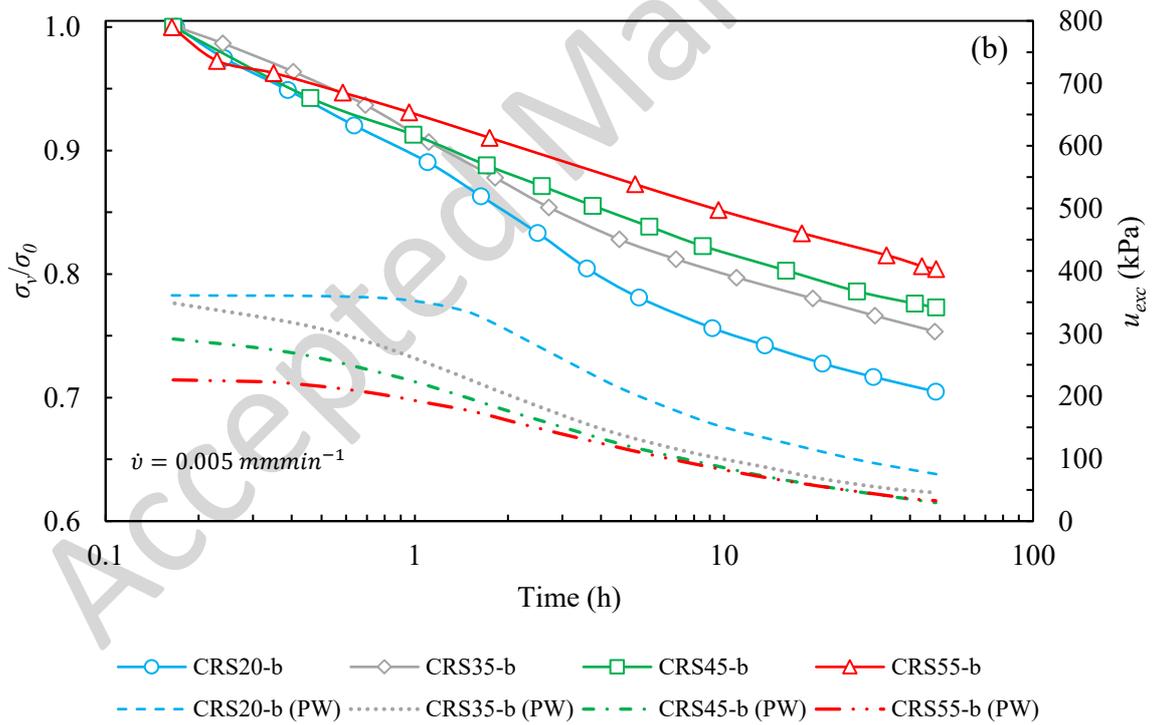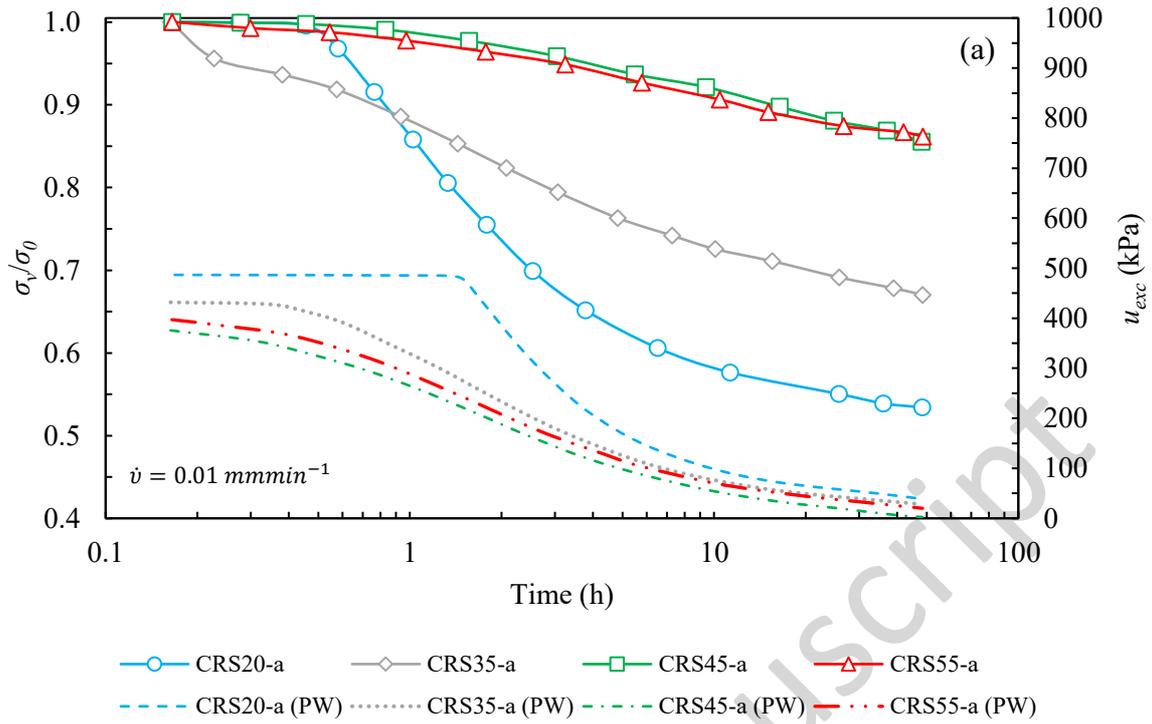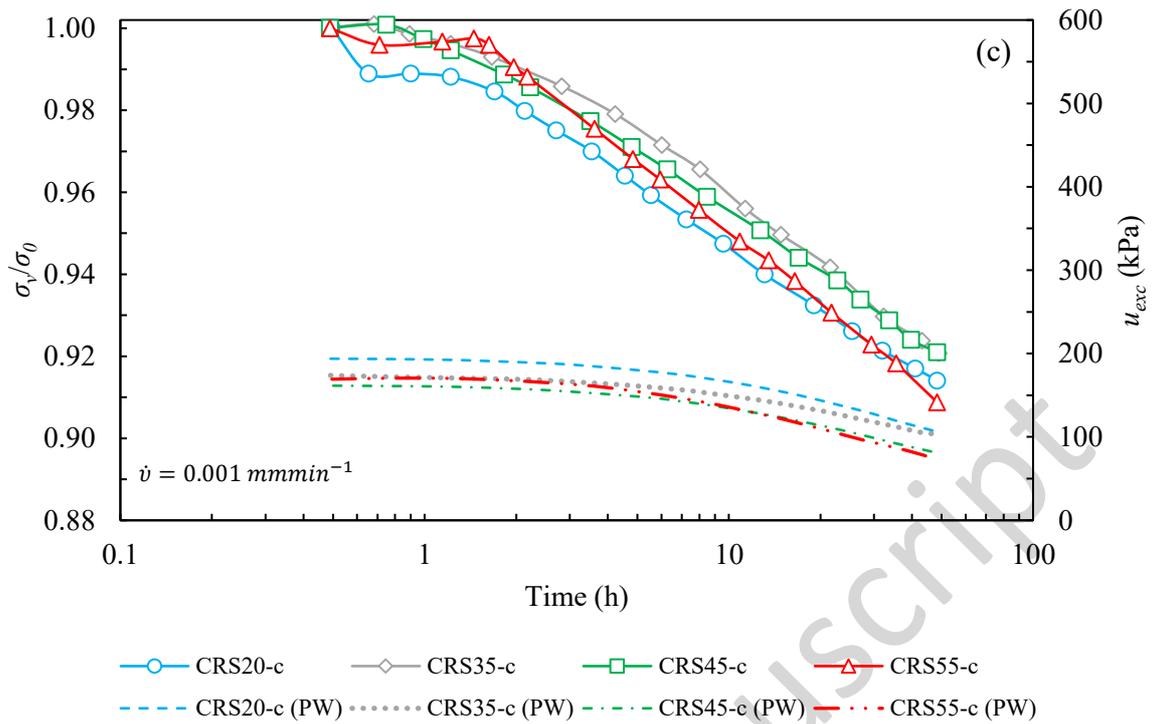
Figure 12 – Temperature effect on stress relaxation in thermal CRS tests at displacement-

rates of: (a) 0.01 mm/min, (b) 0.005 mm/min, and (c) 0.001 mm/min
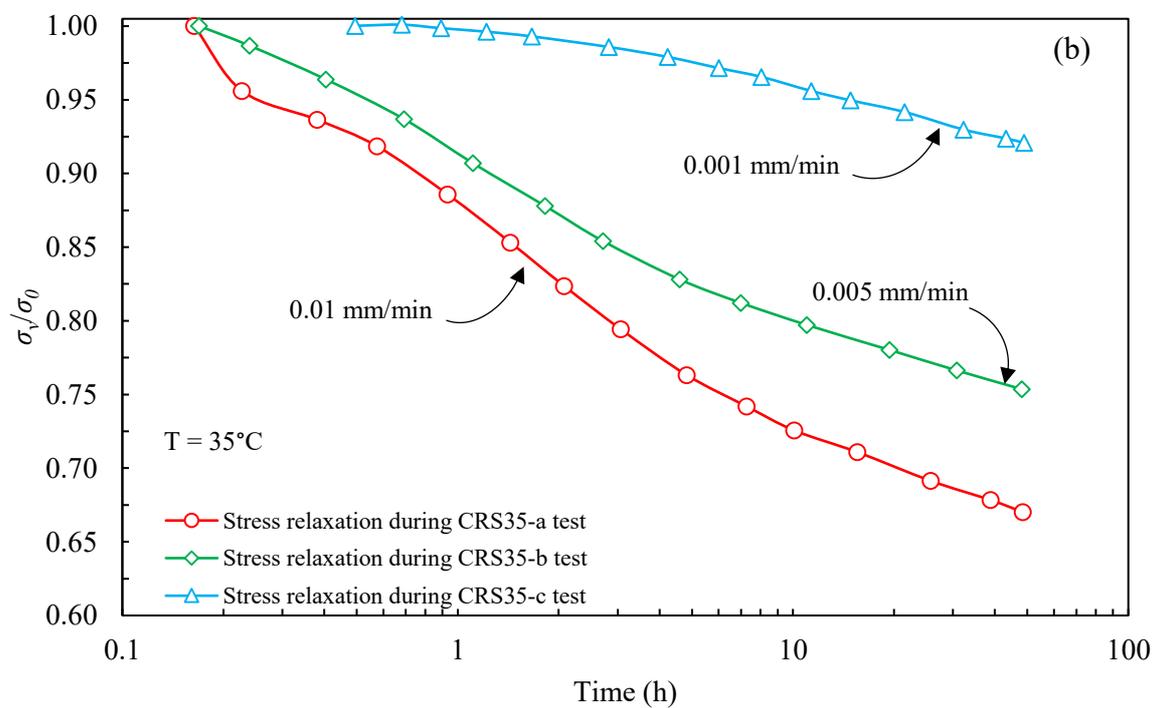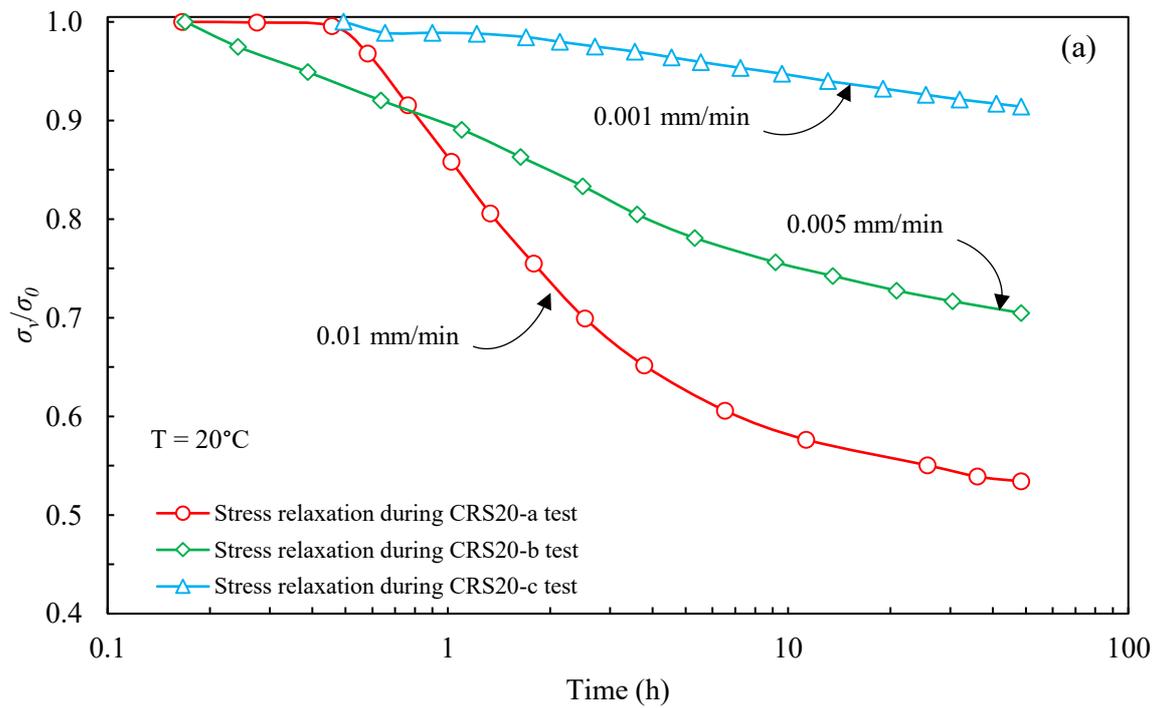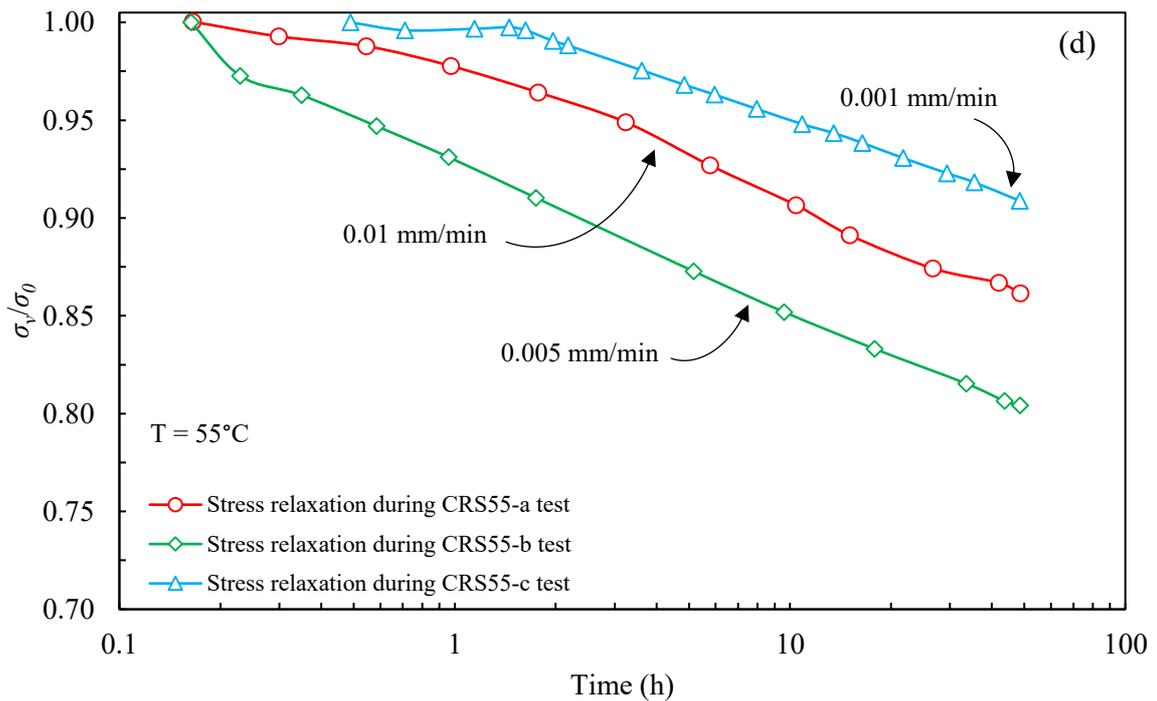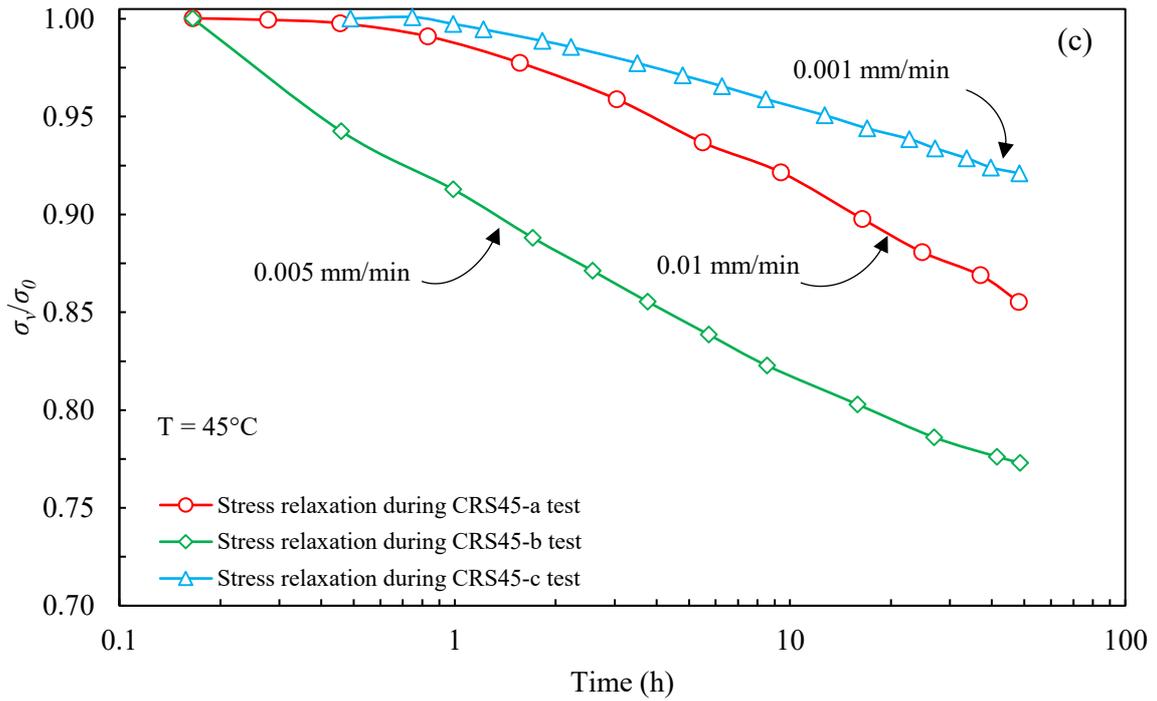
Figure 13 – Displacement-rate effect on stress relaxation in thermal CRS tests at temperatures

of: (a) 20°C, (b) 35°C, (c) 45°C, and (d) 55°C

The variation of relaxation coefficient (R_α) with temperature and displacement-rate is presented in Figure 14. The values of R_α obtained from CRS-a and CRS-b tests decrease approximately linearly with temperature, with the faster displacement-rate (CRS-a) tests producing higher R_α during the 48-hour relaxation period than those tests carried out at the intermediate displacement rate. However, when the displacement-rate decreases in the CRS-c (0.001 mm/min) tests, the trend of R_α alters and shows values to be increasing with temperature. With prolonged loading stage during the CRS-c tests, additional bonding at inter-particle contacts may develop due to the aging effect. The additional inter-particle forces may interrupt the process of stress relaxation. This is evidenced in Table 4, where the variations of relaxation parameters $\Delta\sigma$, $\Delta\sigma/\sigma_0$, and ξ for this set of experiments do not follow a trend. At particle level, the aging bonds may also interrupt or even reverse the migration of pore-water to inter-aggregate space resulting in a slight reduction in R_α values. This is, however, just a possible mechanism based on limited data. Microstructural observations using environmental scanning electron microscope could shed more light on the validity of this hypothesis. At a constant temperature, higher strain energy could be stored within the specimen with increase in pre-relaxation displacement rate $(\dot{v})$, resulting in higher R_α values. Figure 14 shows that as the temperature reaches 55°C, the values of R_α are in the range of 0.030–0.035. Furthermore, a decrease in $\dot{v}$ by a factor of 10, i.e. from 0.01 to 0.001 mm/min, causes the R_α values to reduce by 55 – 11% with temperature increase. In fact, at lower temperatures, the effect of pre-relaxation loading rate seems to be predominant, resulting in significant variation of R_α. The impact of $\dot{v}$ is somehow balanced at higher temperatures (55°C) resulting in a relatively constant R_α values. More experiments under the higher range of temperatures and loading rates are required to validate this hypothesis.
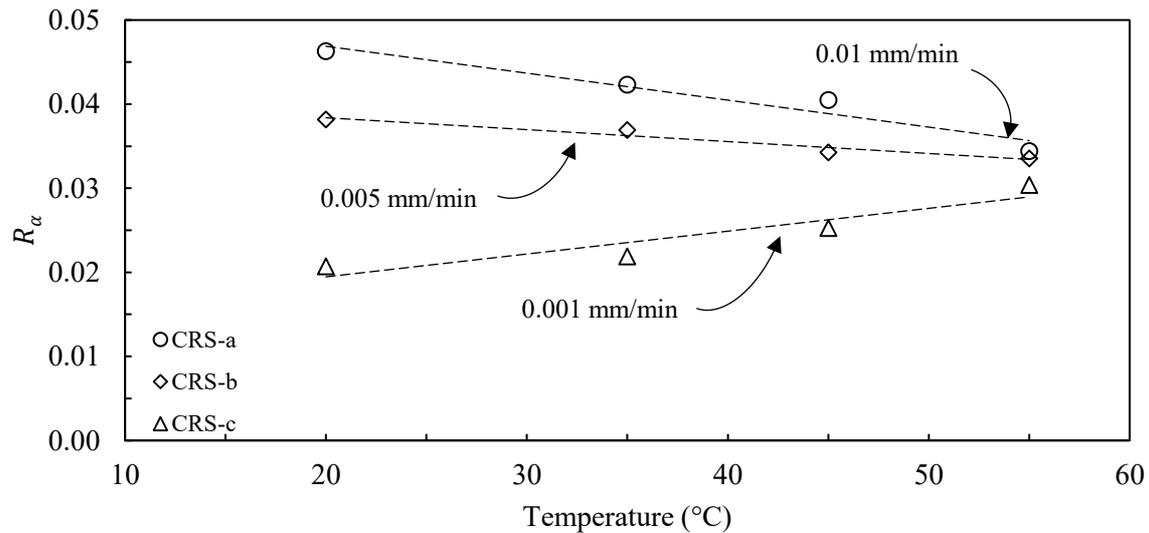
Figure 14 – Variation of R_α with temperature and pre-relaxation displacement-rate

For the fast, intermediate, and slow pre-relaxation displacement-rates, the values of R_α fell within a range of 0.034–0.046, 0.034–0.038, and 0.021–0.030 respectively. The values of $\alpha = C_\alpha/C_c^*$ ratio obtained from MSL oedometer tests fell within a range of 0.026–0.046. This range, with a good approximation, complies with the R_α range of 0.034–0.046 obtained from fast displacement-rate (CRS-a) tests (Figure 15). This further validates the $R_\alpha = \alpha$ correlation for the thermally influenced saturated reconstituted specimens tested in this study. Since this correlation has already been validated for unsaturated reconstituted soft soils (Bagheri, 2018; Bagheri et al., 2019b) and typical saturated reconstituted soft soils (Yin et al., 2014), it is reasonable to suggest time-consuming conventional MSL oedometer tests could be replaced with relatively faster CRS compression-relaxation tests for derivation of time-dependent soil parameters such as C_α.
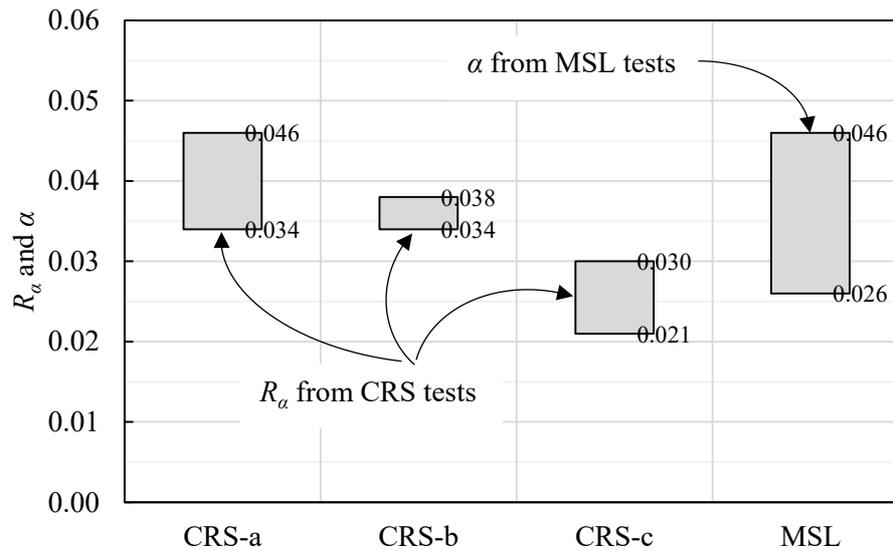
Figure 15 – The range of R_α and α obtained from CRS and MSL tests

Conclusions

To study the effect of temperature on the compressibility, creep and stress relaxation behaviour of clays, thermo-mechanical one-dimensional MSL and CRS tests were carried out on saturated reconstituted LC specimens obtained from London's Bank Station project upgrade. Based on the results of the tests, the following conclusions can be drawn:

- The values of compression index (C_c) vary slightly with temperature change in MSL tests. However, the results of CRS tests revealed an approximately linear reduction in C_c values with increase in temperature within the range of applied stresses and temperatures.

- Temperature has a notable impact on creep index especially at higher stress levels and higher temperatures in the post yield region. This can be attributed to microstructural variations caused by pore-water transfer to inter-aggregate space. However, with scattered data, especially in the elastic domain, it is not possible to make a firm conclusion as to whether temperature cause an increase or decrease in C_α.

30

- At a constant temperature, a decrease in pre-relaxation displacement rate ($\dot{v}$) by a factor of 10 can cause a reduction in coefficient of stress relaxation (R_α) by 55% at lower temperatures (20 ºC) and 11% at higher temperatures (55 ºC).

- The $R_\alpha = \alpha$ correlation can be observed as valid for thermally influenced reconstituted saturated clays in this study. However, more experiments under higher ranges of temperatures and loading rates are required to validate this hypothesis.

- Derivation of time-dependent soil parameters based on relatively fast CRS compression-relaxation tests sounds promising and an alternative to conventional oedometer tests.

The results obtained from this study can potentially provide useful information for calibration of rate-dependent thermo-mechanical soil models for simulation of the behaviour of energy geo-structures under varying temperatures and time. Further work should be performed to investigate the impact of slow displacement-rates on the creep behaviour under higher temperatures.

Data Availability Statement

All data, models, and code generated or used during the study appear in the submitted article.

List of Symbols

The following symbols are used in this paper:

e	=	void ratio
e_0	=	initial void ratio
t	=	time
u_{exc}	=	excess pore-water pressure
w_0	=	initial gravimetric water content
w_L	=	liquid limit
w_P	=	plastic limit
C_c	=	compression index
C_c^*	=	incremental compression index
C_r	=	reloading index
C_r^*	=	incremental reloading index
C_s	=	swelling index
C_α	=	incremental creep index
D	=	grain size
G_s	=	specific gravity
I_P	=	plasticity index
m_c	=	slope of compression curve
R_α	=	coefficient of stress-relaxation
α	=	represents the ratio C_α/C_c
ε_a	=	axial strain
$\dot{v}$	=	displacement-rate
σ_0	=	pre-relaxation total vertical stress
σ_p	=	yield vertical net stress
σ_p'	=	apparent preconsolidation pressure
σ_v	=	applied vertical total stress
σ_s	=	residual total vertical stress
σ_v'	=	vertical effective stress
$\Delta\sigma$	=	relaxed stress
ξ	=	residual stress ratio
LC	=	London clay
LPT	=	linear potentiometric transducer
MSL	=	multi-staged loading
NCL	=	normal compression line
CRS	=	constant rate of strain
1D	=	one-dimensional
PPR	=	pore-water ratio

References

Abuel-Naga, H., Bergado, D., Bouazza, A. and Ramana, G. (2007). Volume change behaviour of saturated clays under drained heating conditions: experimental results and constitutive modeling. *Canadian Geotechnical Journal*, 44: 942-956.

ASTM. (2006). Standard test method for one-dimensional consolidation properties of saturated cohesive soils using controlled-strain loading. ASTM-D4186, West Conshohoken, PA: ASTM.

Bagheri, M. (2018). Experimental investigation of the time- and rate-dependent behaviour of unsaturated clays. Ph.D. thesis, Dept. of Civil Engineering, Univ. of Nottingham.

Bagheri, M., Mousavi Nezhad, M. and Rezania, M. (2019a). A CRS oedometer cell for unsaturated and non-isothermal tests. *Geotechnical Testing Journal*, 43(1): 20-37.

Bagheri, M., Rezania, M. and Mousavi Nezhad, M. (2019b). Rate dependency and stress relaxation of unsaturated Clays. *International Journal of Geomechanics*, 19: 04019128.

Bagheri, M., and Rezania, M. (2021). Geological and geotechnical characteristics of London clay from the Isle of Sheppey. *Geotechnical and Geological Engineering*, 39: 1701-1713

Boudali, M., Leroueil, S., and Srinivasa Murthy, B. R. (1994). Viscous behaviour of natural clays. In Proceedings of the 13th International Conference on Soil Mechanics and Foundation Engineering, New Delhi, A.A. Balkema, Rotterdam, The Netherlands. Vol. 1, pp. 411-416.

Campanella, R. G. and Mitchell, J. K. (1968). Influence of temperature variations on soil behavior. *Journal of the Soil Mechanics and Foundations Division*, 94: 709-734.

Chen, Z. J., Zhao, R. D., Chen, W. B., Wu, P. C., Tin, J. H., and Feng, W. Q. (2023) Effects of temperature on the time-dependent compression and shear behaviour of a soft marine clayey soil. Engineering Geology, 314, 107005.

Cheng, Q., Zhou, C., Ng, C. W. W., and Tang, C. S. (2020). Effects of soil structure on thermal softening of yield stress. *Engineering Geology*, 269, 105544.

Delage, P., Sultan, N., & Cui, Y. J. (2000). On the thermal consolidation of Boom clay. *Canadian Geotechnical Journal*, 37(2), 343-354.

Di Donna, A. and Laloui, L. (2015). Response of soil subjected to thermal cyclic loading: experimental and constitutive study. *Engineering Geology*, 190: 65-76.

Favero, V., Ferrari, A. and Laloui, L. (2016). Thermo-mechanical volume change behaviour of Opalinus Clay. *International Journal of Rock Mechanics and Mining Sciences*, 90: 15-25.

Jarad, N. (2016). Temperature impact on the consolidation and creep behaviour of compacted clayey soils. PhD Thesis, Université de Lorraine.

Jarad, N., Cuisinier, O. and Masrouri, F. (2019). Effect of temperature and strain rate on the consolidation behaviour of compacted clayey soils. *European Journal of Environmental and Civil Engineering*, 23: 789-806.

Kaddouri, Z., Cuisinier, O. and Masrouri, F. (2019). Influence of effective stress and temperature on the creep behavior of a saturated compacted clayey soil. *Geomechanics for Energy and the Environment*, 17: 106-114.

Ladanyi, B. and Benyamina, M. (1995). Triaxial relaxation testing of a frozen sand. *Canadian Geotechnical Journal*, 32: 496-511.

Lahoori, M., Rosin-Paumier, S. and Masrouri, F. (2021). Effect of monotonic and cyclic temperature variations on the mechanical behavior of a compacted soil. *Engineering Geology*, 290: 106195.

Li, Y., Dijkstra, J. and Karstunen, M. (2018). Thermomechanical creep in sensitive clays. *Journal of Geotechnical and Geoenvironmental Engineering*, 144: 04018085.

Loria, A. F. R. and Coulibaly, J. B. (2021). Thermally induced deformation of soils: A critical overview of phenomena, challenges and opportunities. *Geomechanics for Energy and the Environment*, 25: 100193.

Marques, M. E. S., Leroueil, S. and Soares De Almeida, M. D. S. (2004). Viscous behaviour of St-Roch-de-l'Achigan clay, Quebec. *Canadian Geotechnical Journal*, 41: 25-38.

Martinez Calonge, D. (2017). Experimental investigation of the thermo-mechanical behaviour and thermal properties of London clay, PhD Thesis, Imperial College London.

McCartney, J. S. and Murphy, K. D. (2017). Investigation of potential dragdown/uplift effects on energy piles. *Geomechanics for Energy and the Environment*, 10, 21-28.

Rezania, M., Bagheri, M. and Mousavi Nezhad, M. (2020) Creep and consolidation of a stiff clay under saturated and unsaturated conditions. *Canadian Geotechnical Journal*, 57(5), 728-741

Rowe, R. K. (2012) Short- and long-term leakage through composite liners. The 7th Arthur Casagrande Lecture. *Canadian Geotechnical Journal*, 49(2), 141-169

Sultan, N., Delage, P. and Cui, Y.J. (2002) Temperature effects on the volume change behaviour of Boom clay. *Engineering geology*, 64(2-3), 135-145

Tidfors, M. and Sällfors, G. (1989). Temperature effect on preconsolidation pressure. *Geotechnical Testing Journal*, 12: 93-97.

Tsutsumi, A. and Tanaka, H. (2012). Combined effects of strain rate and temperature on consolidation behavior of clayey soils. *Soils and Foundations*, 52: 207-215.

Yin, Z.Y., Zhu, Q.Y., Yin, J.H. and Ni, Q. (2014). Stress relaxation coefficient and formulation for soft soils. *Géotechnique Letters*, 4: 45-51.